LETTERS

# Bile acids induce energy expenditure by promoting intracellular thyroid hormone activation

Mitsuhiro Watanabe[1]*, Sander M. Houten[1]*, Chikage Mataki[1], Marcelo A. Christoffolete[2], Brian W. Kim[2], Hiroyuki Sato[1], Nadia Messaddeq[1], John W. Harney[2], Osamu Ezaki[3], Tatsuhiko Kodama[4], Kristina Schoonjans[1], Antonio C. Bianco[2] & Johan Auwerx[1,5]

**While bile acids (BAs) have long been known to be essential in dietary lipid absorption and cholesterol catabolism, in recent years an important role for BAs as signalling molecules has emerged. BAs activate mitogen-activated protein kinase pathways[1,2], are ligands for the G-protein-coupled receptor (GPCR) TGR5[3,4] and activate nuclear hormone receptors such as farnesoid X receptor α (FXR-α; NR1H4)[5–7]. FXR-α regulates the enterohepatic recycling and biosynthesis of BAs by controlling the expression of genes such as the short heterodimer partner (SHP; NR0B2)[8,9] that inhibits the activity of other nuclear receptors. The FXR-α-mediated SHP induction also underlies the downregulation of the hepatic fatty acid and triglyceride biosynthesis and very-low-density lipoprotein production mediated by sterol-regulatory-element-binding protein 1c[10]. This indicates that BAs might be able to function beyond the control of BA homeostasis as general metabolic integrators. Here we show that the administration of BAs to mice increases energy expenditure in brown adipose tissue, preventing obesity and resistance to insulin. This novel metabolic effect of BAs is critically dependent on induction of the cyclic-AMP-dependent thyroid hormone activating enzyme type 2 iodothyronine deiodinase (D2) because it is lost in *D2*$^{-/-}$ mice. Treatment of brown adipocytes and human skeletal myocytes with BA increases D2 activity and oxygen consumption. These effects are independent of FXR-α, and instead are mediated by increased cAMP production that stems from the binding of BAs with the G-protein-coupled receptor TGR5. In both rodents and humans, the most thermogenically important tissues are specifically targeted by this mechanism because they coexpress D2 and TGR5. The BA–TGR5–cAMP–D2 signalling pathway is therefore a crucial mechanism for fine-tuning energy homeostasis that can be targeted to improve metabolic control.**

To characterize the metabolic effects of BAs, we fed C57BL/6J mice on a high-fat (HF) diet supplemented with cholic acid (CA) at 0.5% w/w. The CA-containing diet was well tolerated and devoid of side effects for up to 47 days. Absence of toxicity was supported by the fact that feeding with CA did not affect food intake, nutrient uptake or serum liver enzymes[11] (Fig. 1a, and not shown). Whereas mice on the HF diet gained more weight than controls, supplementation of the HF diet with CA reduced weight gain comparably to that in chow-fed animals (Fig. 1b). Supplementation of chow with CA had no effect on gain in body weight (ref. 11 and not shown). The changes in weight gain reflect mainly modifications in adiposity: epididymal white adipose tissue (WAT), mesenteric WAT and intrascapular brown adipose tissue (BAT) of HF-fed animals were significantly increased in weight. BAT of HF-fed animals was paler, indicative of decreased metabolic activity and increased fat accumulation. In addition, there was an expansion of WAT surrounding the BAT. Diet supplementation with CA completely prevented the HF-induced changes in adipose mass and morphology (Fig. 1c and Supplementary Fig. S1a). Diet supplementation with CA reversed 120 days of diet-induced weight gain (Fig. 1d). When obese mice were switched to an HF diet containing CA (F-FA), they normalized body weight within 30 days, an effect that was fully accounted for by a decrease in WAT mass (Fig. 1e). Besides preventing and reversing diet-induced obesity, CA also improved glucose tolerance in C57BL/6J mice with diet-induced obesity (ref. 11 and Supplementary Fig. S1b). In an independent experiment, C57BL/6J mice were fed on an HF diet supplemented with the synthetic FXR-α agonist GW4064, but no protective effect against diet-induced obesity was observed (Fig. 1f). The addition of CA to chow also decreased the obesity in KK-A$^{y}$ mice, which was explained by a decrease in WAT mass. This decrease in body weight improved glucose tolerance (Supplementary Fig. S1c). The effects of CA feeding on energy homeostasis coincided with an increase in BA pool size and serum BA levels and a major change in BA composition (Fig. 1g). CA, tauroCA (TCA), deoxyCA (DCA) and taurodeoxyCA (TDCA) were markedly increased. These changes are likely to influence the different BA signalling pathways. These results show that a CA diet prevents and reverses fat accumulation and associated metabolic defects by means of a mechanism that does not depend solely on FXR-α.

With indirect calorimetry, higher $CO_2$ production and $O_2$ consumption were evident in animals fed on an HF diet containing CA when compared with animals on HF diet or chow (Fig. 2a), indicating increased energy expenditure. CA feeding accentuated the HF-induced decrease in the respiratory quotient (RQ), proving that CA increased fat oxidation. To identify the site(s) responsible for the increased energy expenditure, we performed a detailed histological analysis of key metabolic tissues. The HF diet caused adipocyte hypertrophy in WAT and BAT that was not observed when the HF diet was supplemented with CA (Supplementary Fig. S2a). Electron microscopic analysis of BAT demonstrated that, in comparison with the HF diet, CA supplementation increased the number of lamellar cristae in the mitochondria, indicating a major role for BAT in CA-induced energy expenditure (Fig. 2b).

We performed a microarray experiment comparing the expression profile in liver and BAT from mice fed on an HF diet or on an HF diet mixed with CA or chenodeoxycholic acid (CDCA). Major changes in hepatic gene expression were related to cholesterol and BA synthesis

[1]Institut de Génétique et Biologie Moléculaire et Cellulaire, CNRS/INSERM/ULP, 1 Rue Laurent Fries, 67404 Illkirch, France. [2]Department of Medicine, Thyroid Section, Division of Endocrinology, Diabetes and Hypertension, Brigham and Women's Hospital and Harvard Medical School, Boston, Massachusetts 02115, USA. [3]Division of Clinical Nutrition, National Institute of Health and Nutrition, 1-23-1 Toyama, Shinjuku-ku, Tokyo 162-8636, Japan. [4]Laboratory for Systems Biology and Medicine, RCAST, University of Tokyo, Tokyo 153-8904, Japan. [5]Institut Clinique de la Souris, 67404 Illkirch, France.
*These authors contributed equally to this work.

but not to energy homeostasis (not shown). In BAT, however, several genes involved in the control of energy expenditure were upregulated by BAs (Supplementary Table 1). We focused on *D2*, whose expression was most affected. D2 converts inactive thyroxine ($T_4$) into active 3,5,3′-tri-iodothyronine ($T_3$)[12] and is a crucial determinant of thyroid hormone receptor saturation in cells in which it is expressed. The vital role of D2 in energy homeostasis is well established in mice, in which BAT adaptive thermogenesis depends on this enzyme[12].

We used quantitative reverse transcriptase-mediated polymerase chain reaction to confirm the induction of *D2* by BAs and to measure messenger RNA levels of genes involved in energy homeostasis and BA signalling in liver, muscle and BAT. For these studies we used organs from the C57BL/6J mice described in Fig. 1a–c. The expression of key genes in energy expenditure such as the *peroxisome-proliferator-activated receptor γ coactivator (PGC)-1α*, *PGC-1β*, *uncoupling protein (UCP)-1*, *UCP-3*, *straight-chain acyl-CoA oxidase 1 (ACO)*, *muscle-type carnitine palmitoyltransferase I (mCPT-I)* and *D2* was significantly increased in BAT after BA feeding (Fig. 2c). Similar changes were not observed in liver or muscle. *FXR-α* and *SHP* expression was not detected in BAT under any of the conditions, whereas we confirmed the induction of SHP by BAs in liver (Fig. 2c)[8,9]. *FGFR-4*, another gene implicated in BA signalling[13], was only expressed to substantial amounts in liver. In addition, treatment with GW4064 did not induce a thermogenic gene response as seen with CA (not shown). These results confirm that BAT is the primary target of the metabolic effects of BAs in mice and that the beneficial effects of BAs on energy homeostasis do not depend solely on FXR-α.

Next we used mice with a targeted disruption of the *D2* gene ($D2^{-/-}$ mice) and littermate controls in a diet-induced obesity study. Wild-type and $D2^{-/-}$ mice gained weight to similar extents, indicating that adaptive thermogenesis was increased sufficiently in $D2^{-/-}$ mice to prevent disproportional weight gain (Fig. 3a). This stands in contrast with the situation of acute exposure to cold, in which $D2^{-/-}$ BAT thermogenesis is insufficient to maintain body temperature and survival is possible only with a major increase in sympathetic activity[14] and mechanical thermogenesis[15]. CA supplementation to the HF diet prevented diet-induced obesity in wild-type mice but had no effect in $D2^{-/-}$ mice (Fig. 3a). Similarly, CA was unable to decrease the weight of the epididymal WAT and BAT in HF-fed $D2^{-/-}$ mice (Fig. 3b). Histological and electron microscopic analysis of BAT showed that combining the HF diet with CA prevented lipid accumulation in BAT of wild-type but not that of $D2^{-/-}$ mice (Fig. 3c and Supplementary Fig. S2b). The lack of alterations in serum $T_4$ and $T_3$ levels in mice fed CA (Supplementary Table 2) confirms the tissue specificity of our findings. Together, these results prove that D2 is an essential mediator in the prevention of diet-induced weight gain by BAs.

Our data led us to focus on FXR-α-independent signalling events stimulated by BAs. *D2* expression is regulated primarily through the cAMP–protein kinase A (PKA) pathway, and a functional cAMP-responsive element (CRE) has been identified in human and mouse *D2* promoter[12]. TGR5 is the only GPCR that has been reported to respond to BAs by the production of cAMP and the subsequent activation of PKA signalling pathways[3,4]. We therefore added CA and DCA and their taurine conjugates (TCA and TDCA) to cells co-transfected with a CRE-driven luciferase reporter and a TGR5 expression plasmid. All tested BAs enhanced luciferase activity in a TGR5-dependent fashion, showing that cAMP production by BAs requires TGR5 (Fig. 3d). The effect of forskolin, an adenylyl cyclase activator, on luciferase activity was independent of TGR5 (Fig. 3d). Physiological concentrations of BAs increased luciferase expression dose dependently in TGR5-transfected cells, proving tight coupling between BA–TGR5 and intracellular PKA signalling (Fig. 3e). *D2* and *TGR5* mRNAs are coexpressed in mouse BAT, which has the highest relative expression level of both genes in the selected mouse tissues tested (Fig. 3f). Expression of *TGR5* and low levels of *D2* mRNAs were also found in brain and thyroid gland, but the latter has no measurable D2 activity[12]. Further proof that BAs signal by means of cAMP–PKA activation comes from elevated cAMP levels in BAT of C57BL/6J and KK-$A^y$ mice fed on a CA diet (Fig. 3g). Taken together, these results indicate that the effects of BAs on BAT could be

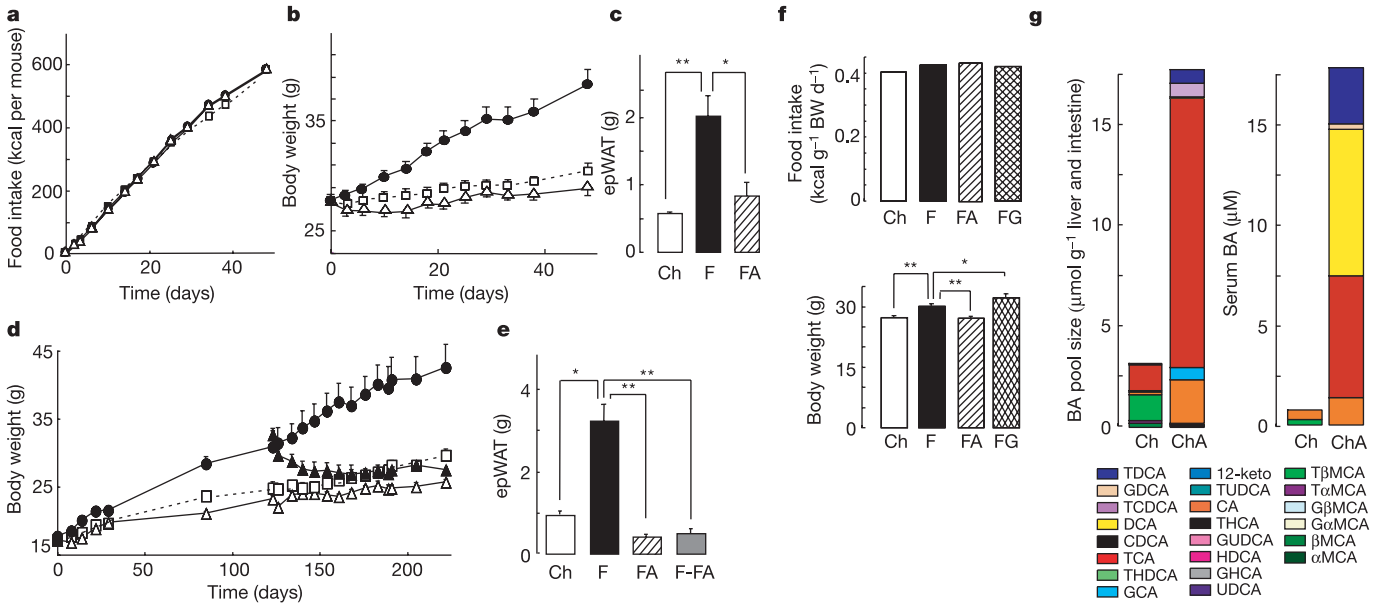


**Figure 1 | CA decreases adiposity of mice fed a HF diet.** **a**, **b**, Change in cumulative food intake (**a**) and body weight (**b**) of C57BL/6J mice over 47 days. Squares, chow (Ch); circles, HF diet (F); triangles, HF diet plus CA (FA). **c**, Comparison of epididymal WAT (epWAT). **d**, Changes of body weight in C57BL/6J mice. After 120 days half of the mice on the HF diet (filled triangles) were switched to HF diet supplemented with CA. Other symbols as in **a**. **e**, Comparison of epWAT weights. F-FA, switched to HF diet supplemented with CA. **f**, Food intake and body weight (BW) of C57BL/6J mice after 1 month on diets containing natural CA or synthetic (GW4064) FXR-α agonist (FG, HF plus GW4064). **g**, Composition of BAs in enterohepatic organs and serum of KK-$A^y$ mice after 21 days on the indicated diets. Abbreviations: Glyco (G), Hyo (H), Urso (U) and Muri (M). Error bars show s.e.m. ChA, chow diet supplemented with cholic acid.

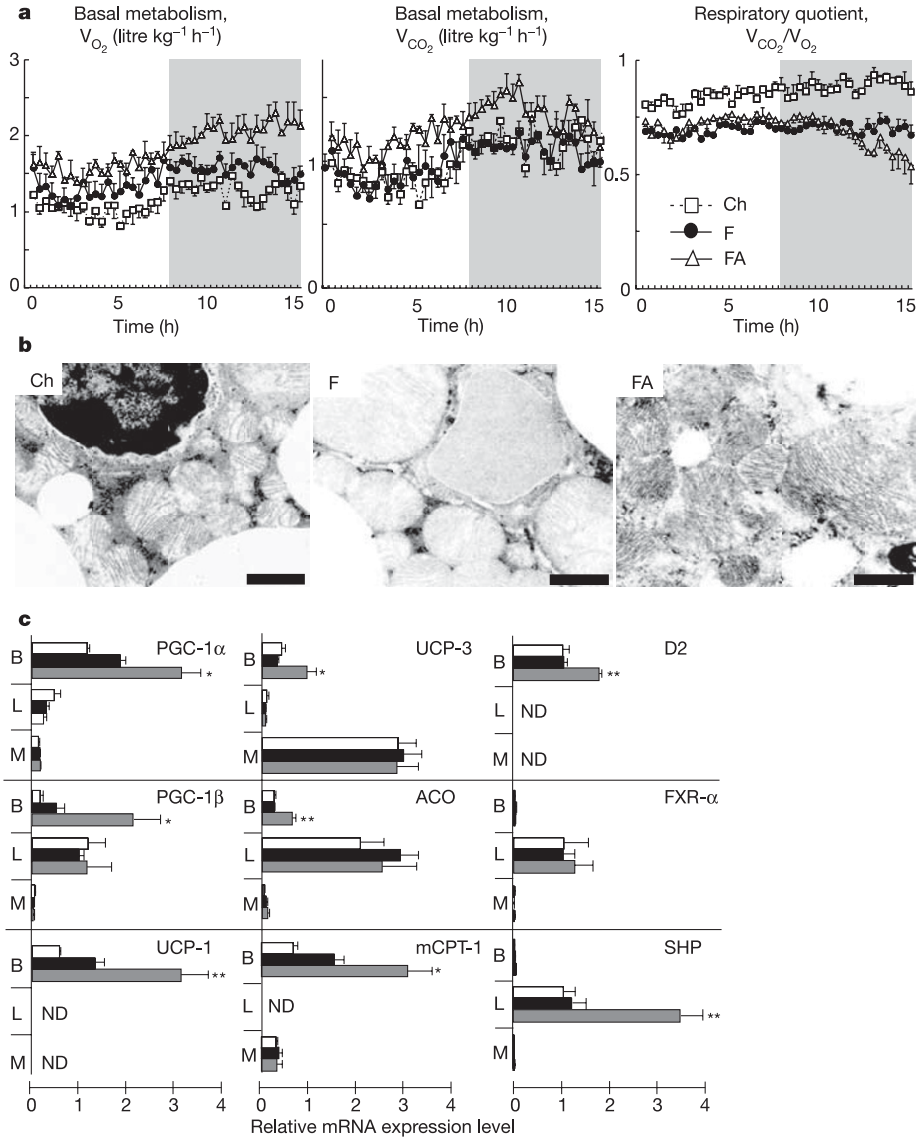


**Figure 2 | CA increases energy expenditure.** **a**, $O_2$ consumption, $CO_2$ production and RQ in mice on different diets for 4 months (C57BL/6J, $n = 3$, age 26 weeks). The acclimation time was 2 h. $O_2$ consumption was normalized to (body weight)$^{0.75}$. The shaded area indicates the dark phase. Squares, chow (Ch); circles, HF diet (F); triangles, HF diet plus CA (FA). **b**, BAT analysis by transmission electron microscopy. Scale bar, 1 μm. **c**, Relative mRNA expression levels of PGC-1α, PGC-1β, UCP-1, UCP-3, ACO, mCPT-I, D2, FXR-α and SHP in BAT (B), liver (L) and muscle (M). ND, not detectable. White bars, chow; black bars, HF diet; grey bars, HF diet plus CA. Error bars show s.e.m.

mediated through the activation of GPCRs, such as TGR5, and the subsequent activation of PKA signalling.

To reproduce the effect of BAs *in vitro*, we isolated BAT cells from C57BL/6J mice fed on either a control or an HF diet. TCA dose-dependently increased *D2* mRNA and D2 activity (Fig. 4a). Interestingly, cells from HF-fed mice were more sensitive to the addition of TCA but also to forskolin (Fig. 4a). This could explain why BAs have major effects on energy homeostasis only when supplementing an HF diet and indicates that besides BAs other factors have a function in the induction of D2. Several different BAs increased cAMP, indicating that this second messenger induces *D2* expression. The FXR-α agonist GW4064 failed to increase cAMP in BAT cells (Fig. 4b). The effect of an HF diet on cAMP production by BAT cells was less pronounced than on *D2* mRNA and D2 activity, indicating that an HF diet influences D2 induction somewhere downstream of the GPCR.

In contrast to rodents, adult humans do not have significant amounts of BAT but express significant levels of *D2* in skeletal muscle[12] (Fig. 4c), an organ of critical importance to energy homeostasis. *TGR5* mRNA was also expressed in human skeletal muscle (Fig. 4c). To investigate whether *D2* expression in human skeletal muscle could be induced by BAs, by analogy with the induction of *D2* expression in BAT in mice, we used primary cultures of human skeletal muscle myoblasts (HSMM) expressing *D2* and high levels of *TGR5* (Fig. 4c). On incubation of HSMM with TCA, we observed a significant and dose-dependent induction of D2 activity (Fig. 4d). Again, the FXR-α agonist GW4064 did not stimulate D2. Major BA species such as CA, TCA, DCA and CDCA increased cAMP levels in a dose-dependent fashion, paralleling the increase in D2 activity (Fig. 4e). However, GW4064 did not increase cAMP levels (Fig. 4e).

We were unable to knock down TGR5 function with several different short interfering RNAs as well as a plasmid encoding a small hairpin RNA. As an alternative approach to demonstrate that the effects of BAs on cAMP levels and D2 activity were mediated by TGR5, we used benzyl 2-keto-6-methyl-4-(2-thienyl)-1,2,3,4-tetrahydropyrimidine-5-carboxylate, a highly selective synthetic TGR5 agonist[16] (Fig. 4f). This TGR5 agonist dose-dependently induced the

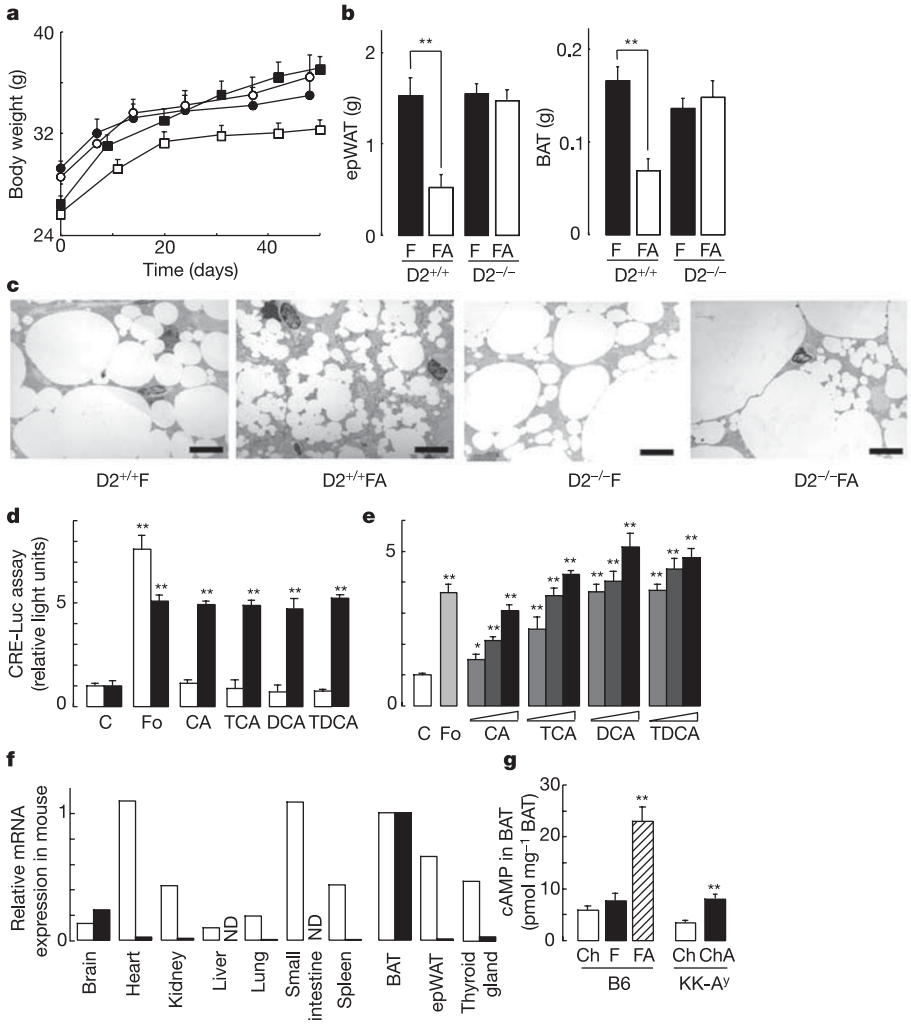


**Figure 3 | BAs signal by means of D2. a**, Body weight change in $D2^{+/+}$ and $D2^{-/-}$ mice over 50 days. Filled squares, $D2^{+/+}$, HF diet (F); open squares, $D2^{+/+}$, HF diet plus CA (FA); filled circles, $D2^{-/-}$, F; open circles, $D2^{-/-}$, FA. **b**, Comparison of the weights of epWAT and BAT. **c**, Osmium-tetroxide-stained BAT was analysed by transmission electron microscopy. Scale bars, 5 μm. **d**, CRE reporter assay in CHO cells transfected with pCRE-Luc and TGR5 expression vector. Concentrations: 100 μM BA, 5 μM forskolin (Fo). C means control. Open bars, vector; filled bars, pTGR5. **e**, CRE reporter assay in CHO cells transfected with pCRE-Luc and TGR5 expression vector in the presence of different concentrations (1.8, 5.5 and 17 μM) of the indicated BAs. **f**, Expression of *TGR5* (open panels) and *D2* (filled panels) in selected mouse tissues. ND, not detectable. **g**, cAMP levels in BAT of C57BL/6J and KK-$A^{y}$ mice after 7 days on the diets. Ch means chow and ChA means chow + CA. Error bars show s.e.m.

activity of a CRE-luciferase reporter in a TGR5-dependent fashion, but TCA was more effective at equimolar concentrations (Fig. 4f). In addition, the TGR5 agonist enhanced D2 activity in HSMM cells, an effect potentiated in the presence of 3-isobutyl-1-methylxanthine (Fig. 4g), indicating that the effects of BAs on D2 activity might be mediated by TGR5.

Finally, we determined the oxygen consumption and extracellular acidification rate in HSMM after treatment with BA. Oxygen consumption is a measure for aerobic mitochondrial oxidation, whereas extracellular acidification rate is a measure for glycolysis, lactate production and anaerobic metabolism. TCA, like $T_3$, elevated cellular oxygen consumption in line with the induction of mitochondrial activity (Fig. 4h). This indicates that TCA induces D2, which converts $T_4$ derived from the fetal bovine serum into $T_3$. In addition, we observed an increase in extracellular acidification rate for both $T_3$ and TCA after 72 h of treatment, which could suggest a limiting reducing capacity caused by oxygen shortage. In combination, these results suggest that BAs increase *D2* mRNA, D2 activity and energy expenditure by means of a TGR5–cAMP-mediated pathway in mouse BAT and HSMM.

Recent observations indirectly support a role for D2 as a determinant of energy expenditure in human skeletal muscle. A functionally significant polymorphism in the D2 gene[17] is strongly associated with decreased whole-body glucose disposal rate, which is determined mainly by muscle glucose uptake[18]. In patients with type 2 diabetes this polymorphism is associated with increased insulin resistance[17].

The pharmacological relevance of the BA–cAMP–D2–$T_3$ pathway is clearly supported by our data, but the same pathway could also be of physiological importance. The extraction of BAs from portal blood by the liver is remarkably efficient (70–90%) and usually remains constant during fasting and digestion[19]. Thus, after a meal, BA levels in the hepatocyte increase and a significant amount of BAs spills over into the systemic circulation. Fasting serum BA levels are usually lower than 5 μM, whereas postprandial levels increase to up to 15 μM (ref. 20), consistent with the concentrations required to stimulate cAMP production and D2 activity in our *in vitro* studies. Thus, the circadian variation in serum BA levels could be a diurnal hormonal signal reflecting food intake and one of the key factors in diet-induced thermogenesis.

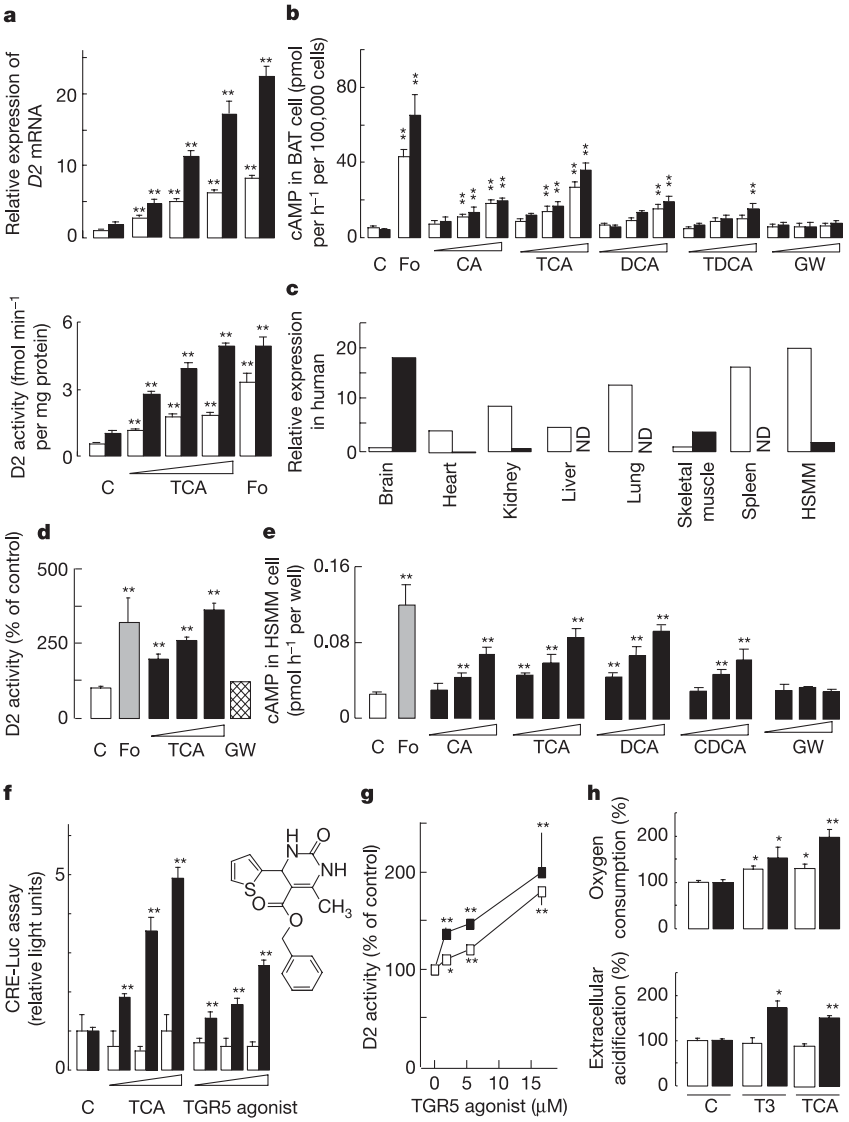


**Figure 4 | *In vitro* effects of BAs.** **a**, *D2* expression (upper panel) and D2 activity (lower panel) in BAT cells from C57BL/6J mice after 14 days on chow (open columns) and HF diet (filled columns). Cells were treated with TCA or forskolin (Fo) (as in Fig. 3e). **b**, Induction of cAMP by BAs in BAT cells (as in Fig. 3e). GW, GW4064 at 1.1, 3.3 and 10 μM. Open columns, chow; filled columns, HF diet. **c**, Expression of *TGR5* (open columns) and *D2* (filled columns) in selected human tissues. ND, not detectable. **d**, Induction of D2 activity in HSMM by TCA (1.3, 4 and 12 μM), GW4064 (3 μM) and forskolin (10 μM). **e**, Induction of cAMP by BAs in HSMM (as in **b**). **f**, CRE reporter assay (as in Fig. 3d). Agonists were used at 1, 3.2 and 10 μM. Open columns, vector; filled columns, pTGR5. The structure of benzyl 2-keto-6-methyl-4-(2-thienyl)-1,2,3,4-tetrahydropyrimidine-5-carboxylate is also shown. **g**, Induction of D2 activity in HSMM by the synthetic TGR5 agonist (1, 5 and 15 μM) in the absence (open columns) or presence (filled columns) of 1 mM IBMX. **h**, Induction of oxygen consumption (upper panel) and extracellular acidification rate (lower panel) in HSMM by 5 μM TCA and 50 nM $T_3$. Open columns, 48 h; filled columns, 72 h. Error bars show s.e.m.

## METHODS

**Materials.** 3-Isobutyl-1-methylxanthine (IBMX), CA, TCA, DCA, TDCA and forskolin were from Sigma. Benzyl 2-keto-6-methyl-4-(2-thienyl)-1,2,3,4-tetrahydropyrimidine-5-carboxylate was synthesized by ChemBridge. GW4064 was a gift from S. Inoue.

**Plasmids.** pCRE-Luc was from Clontech. NIH MGC Clone Collection MGC:40597 (pTGR5) was from Invitrogen.

**Cell culture, transient transfection and luciferase assays.** The Chinese hamster ovary cell line was obtained from ATCC. Cells were maintained in α-MEM with 10% (v/v) fetal bovine serum at 37 °C in a humidified atmosphere of 5% $CO_2$/95% air; 70–80% confluent cells were transfected in 96-well plates with Lipofectamine 2000 (Invitrogen). Each well contained 50 ng of luciferase reporter (pCRE-Luc) plasmid and 200 ng of TGR5 expression plasmid or the empty expression vector. After incubation for 6 h with DNA–Lipofectamine complexes, the transfection medium was exchanged for DMEM medium containing 0.1% BSA (Sigma). After incubation for 18 h, the medium was exchanged for 0.1% BSA–DMEM medium with BAs or forskolin. Stock solutions of these compounds were prepared in dimethylsulphoxide. After incubation for 6 h with the different compounds, cells were lysed and used for luciferase determination.

**mRNA expression analysis.** mRNA expression levels were analysed in cDNA synthesized from total mRNA with the real-time polymerase chain reaction as described[10]. The sequences of the primer sets used are available at http://www-igbmc.u-strasbg.fr/recherche/Dep_GPSN/Eq_JAuwe/Publi/Paper.html.

**Cell culture of HSMM.** HSMM were obtained from Cambrex and were cultured in accordance with the supplier's instructions. D2 activity measurements were performed after incubation for 16 h with the indicated compounds. For cAMP measurements, cells were preincubated for 12 h in Opti-MEM (Life Technologies) supplemented with 1 mM IBMX. Then medium was changed and cells were incubated for a further 1 h in Opti-MEM with 1 mM IBMX, after which the medium was replaced by Opti-MEM with 1 mM IBMX and the indicated compounds. After 30 min, cells were lysed for cAMP analysis.

**Oxygen consumption and extracellular acidification rate.** HSMM were seeded in 24-well microplates. Quadruplicate wells were treated with 50 nM $T_3$, 5 μM

TCA or vehicle. Cells were assayed in the CellDoctor prototype instrument from Seahorse Bioscience to perform non-destructive, time-resolved measurements of oxygen consumption rate and extracellular acidification rate (ECAR). Immediately before measurement, medium was replaced with non-buffered pH 7.4 speciality medium (1:1 saline and 2 × DMEM) to facilitate rapid ECAR measurement. Three successive 10-min measurements were performed simultaneously at 5-min intervals in the quadriplicate wells. Immediately after measurement, total cell number was counted with a Beckman Coulter ViCell.

**Cell isolation and cAMP generation in brown adipocytes.** Freshly dispersed brown adipocytes were isolated as described[21], with some modifications[22]. Cell integrity was confirmed by Trypan blue exclusion in the absence of BSA. Cells were counted and diluted to 500,000 cells $ml^{-1}$. Diluted cells were incubated for 1 h in the presence of 500 μM IBMX and 0.3 U $ml^{-1}$ adenosine deaminase. Responses to forskolin and BAs were generated as described with the experiment. All additions were diluted in the incubation medium (DMEM/F12). Incubation was terminated by the addition of perchloric acid to a final concentration of 6.0%.

**Animals.** Male C57BL/6J and KK-$A^y$ mice, 6–7 weeks of age, were obtained from Charles River Laboratories France and CLEA Japan, respectively. $D2^{-/-}$ mice were originally bred to a C57BL/6J-129SV background[15] and backcrossed for five generations to C57BL/6J. The composition of the different diets was as described[10]. GW4064 was mixed with the HF diet at 180 mg $kg^{-1}$ of food. On the basis of their daily food intake, this resulted in a daily dose of 15 mg $kg^{-1}$ body weight. The mice were fasted for 4 h before blood and tissues were harvested for RNA isolation, lipid measurements and histology. Oxygen consumption was measured with the Oxymax apparatus (Columbus Instruments)[23]. Histological analysis and transmission electron microscopy were performed as described[23].

**Clinical biochemistry and evaluation of glucose, lipid and BA homeostasis.** An oral glucose tolerance test was performed in animals that had been fasted overnight. Glucose was administered by gavage at a dose of 2 g $kg^{-1}$. An intraperitoneal insulin tolerance test was performed in animals fasted for 4 h. Insulin was injected at a dose of 0.75 U $kg^{-1}$ body weight. Glucose was quantified with the Maxi Kit Glucometer 4 (Bayer Diagnostic) or Glucose RTU (bioMérieux Inc.). Plasma insulin concentrations were measured by ELISA (Cristal Chem Inc.). D2 activity was assayed as described[24]. cAMP was measured with the cAMP-Screen system (Applied Biosystems) or a solid-phase radioimmunoassay kit (NEN). BAs in plasma and enterohepatic organs of fed mice were determined as described in ref. 25.

**Statistical analysis.** Statistical differences were determined by either ANOVA or Student's *t*-test. Statistical significance is displayed as $P < 0.05$ (one asterisk) or $P < 0.01$ (two asterisks).

**Received 11 April; accepted 19 October 2005.**
**Published online 8 January 2006.**

1. Gupta, S., Stravitz, R. T., Dent, P. & Hylemon, P. B. Down-regulation of cholesterol 7α-hydroxylase (CYP7A1) gene expression by bile acids in primary rat hepatocytes is mediated by the c-Jun N-terminal kinase pathway. *J. Biol. Chem.* **276,** 15816–15822 (2001).
2. Qiao, L. *et al.* Bile acid regulation of C/EBPβ, CREB, and c-Jun function, via the extracellular signal-regulated kinase and c-Jun $NH_2$-terminal kinase pathways, modulates the apoptotic response of hepatocytes. *Mol. Cell. Biol.* **23,** 3052–3066 (2003).
3. Kawamata, Y. *et al.* A G protein-coupled receptor responsive to bile acids. *J. Biol. Chem.* **278,** 9435–9440 (2003).
4. Maruyama, T. *et al.* Identification of membrane-type receptor for bile acids (M-BAR). *Biochem. Biophys. Res. Commun.* **298,** 714–719 (2002).
5. Makishima, M. *et al.* Identification of a nuclear receptor for bile acids. *Science* **284,** 1362–1365 (1999).
6. Parks, D. J. *et al.* Bile acids: natural ligands for an orphan nuclear receptor. *Science* **284,** 1365–1368 (1999).
7. Wang, H., Chen, J., Hollister, K., Sowers, L. C. & Forman, B. M. Endogenous bile acids are ligands for the nuclear receptor FXR/BAR. *Mol. Cell* **3,** 543–553 (1999).
8. Goodwin, B. *et al.* A regulatory cascade of the nuclear receptors FXR, SHP-1, and LRH-1 represses bile acid biosynthesis. *Mol. Cell* **6,** 517–526 (2000).
9. Lu, T. T. *et al.* Molecular basis for feedback regulation of bile acid synthesis by nuclear receptors. *Mol. Cell* **6,** 507–515 (2000).
10. Watanabe, M. *et al.* Bile acids lower triglyceride levels via a pathway involving FXR, SHP, and SREBP-1c. *J. Clin. Invest.* **113,** 1408–1418 (2004).
11. Ikemoto, S. *et al.* Cholate inhibits high-fat diet-induced hyperglycemia and obesity with acyl-CoA synthetase mRNA decrease. *Am. J. Physiol.* **273,** 37–45 (1997).
12. Bianco, A. C., Salvatore, D., Gereben, B., Berry, M. J. & Larsen, P. R. Biochemistry, cellular and molecular biology, and physiological roles of the iodothyronine selenodeiodinases. *Endocr. Rev.* **23,** 38–89 (2002).
13. Holt, J. A. *et al.* Definition of a novel growth factor-dependent signal cascade for the suppression of bile acid biosynthesis. *Genes Dev.* **17,** 1581–1591 (2003).
14. Christoffolete, M. A. *et al.* Mice with targeted disruption of the Dio2 gene have cold-induced overexpression of the uncoupling protein 1 gene but fail to increase brown adipose tissue lipogenesis and adaptive thermogenesis. *Diabetes* **53,** 577–584 (2004).
15. de Jesus, L. A. *et al.* The type 2 iodothyronine deiodinase is essential for adaptive thermogenesis in brown adipose tissue. *J. Clin. Invest.* **108,** 1379–1385 (2001).
16. Hinuma, S. *et al.* Screening method (method for the screening of agonists or antagonists of TGR5). Japanese patent 2003–380574 (P2005–21151A (JP)). 2005.
17. Canani, L. H. *et al.* The type 2 deiodinase A/G (Thr92Ala) polymorphism is associated with decreased enzyme velocity and increased insulin resistance in patients with type 2 diabetes mellitus. *J. Clin. Endocrinol. Metab.* **90,** 3472–3478 (2005).
18. Mentuccia, D. *et al.* Association between a novel variant of the human type 2 deiodinase gene Thr92Ala and insulin resistance: evidence of interaction with the Trp64Arg variant of the beta-3-adrenergic receptor. *Diabetes* **51,** 880–883 (2002).
19. Cohen, D. E. in *Hepatology: A Textbook of Liver Disease* (eds Zakim, D. & Boyer, T. D.) 1713–1743 (Saunders, Philadelphia, 2003).
20. Everson, G. T. Steady-state kinetics of serum bile acids in healthy human subjects: single and dual isotope techniques using stable isotopes and mass spectrometry. *J. Lipid Res.* **28,** 238–252 (1987).
21. Fain, J. N., Reed, N. & Saperstein, R. The isolation and metabolism of brown fat cells. *J. Biol. Chem.* **242,** 1887–1894 (1967).
22. Branco, M., Ribeiro, M., Negrao, N. & Bianco, A. C. 3,5,3′-Triiodothyronine actively stimulates UCP in brown fat under minimal sympathetic activity. *Am. J. Physiol.* **276,** E179–E187 (1999).
23. Picard, F. *et al.* SRC-1 and TIF2 control energy balance between white and brown adipose tissues. *Cell* **111,** 931–941 (2002).
24. Curcio, C. *et al.* The human type 2 iodothyronine deiodinase is a selenoprotein highly expressed in a mesothelioma cell line. *J. Biol. Chem.* **276,** 30183–30187 (2001).
25. Sakakura, H. *et al.* Simultaneous determination of bile acids in rat bile and serum by high-performance liquid chromatography. *J. Chromatogr.* **621,** 123–131 (1993).

**Supplementary Information** is linked to the online version of the paper at www.nature.com/nature.

**Acknowledgements** We thank S. Iwasaki, A. Izumi, T. Taniguchi, K. Sakai, G. Tsujimoto, Y. Kawamata, H. Overmars, T. Sorg, M.-F. Champy and the staff of the Institut Clinique de la Souris for technical assistance and discussions. We also thank Seahorse Bioscience for the collaborative studies of oxygen consumption and extracellular acidification rate in the human skeletal myocytes. Work in the laboratories of the authors is supported by grants from CNRS, INSERM, ULP, FRM, the Hôpital Universitaire de Strasbourg, the NIH, EMBO and the EU.

**Author Contributions** M.W. and S.M.H. were involved in project planning, experimental work and data analysis; C.M., M.A.C., B.W.K., H.S., N.M., J.W.H., O.E., T.K. and K.S. performed experimental work; and A.C.B. and J.A. were involved in project planning and data analysis.

**Author Information** Reprints and permissions information is available at npg.nature.com/reprintsandpermissions. The authors declare no competing financial interests. Correspondence and requests for materials should be addressed to J.A. (auwerx@igbmc.u-strasbg.fr).